ELSEVIER

Wave Motion 27 (1998) 117–136

WAVE MOTION

Nonlinear waves in an inextensible flexible helix

V. Krylov *, R. Parnes, L. Slepyan

Department of Solid Mechanics, Materials and Structures Faculty of Engineering, Tel Aviv University, 69978 Tel Aviv, Israel

Received 25 September 1996; received in revised form 20 August 1997; accepted 4 September 1997

Abstract

The complete analytical solution of the governing nonlinear vector equations is found which describes periodic and solitary propagating-rotating waves in an initially helical fiber. A detailed description of various types of these waves is given. The solitary wave velocity is found to be proportional to the square root of the amplitude of the internal force, and the effective wave length is shown to be independent of the amplitude. The essential influence of the rigid body rotation of the helix on the wave shape is shown. Axial and angular momenta are determined as well. Copyright © 1998 Elsevier Science B.V.

1. Introduction and governing equations

We consider an infinite inextensible, flexible fiber of constant mass density ρ per unit length whose equation of motion and inextensibility condition are respectively

$$\frac{\partial}{\partial S}\left[F(S,t)\,\frac{\partial \mathcal{R}(S,t)}{\partial S}\right] = \rho\frac{\partial^2 \mathcal{R}(S,t)}{\partial t^2}, \tag{1}$$

$$\left|\frac{\partial \mathcal{R}}{\partial S}\right| = 1. \tag{2}$$

Here F is a nonnegative internal tension force, $\mathcal{R}$ is the position vector, S is the coordinate measured along the fiber and t is time. The nonlinear vector equations governing the dynamics of the fiber are of particular interest in the case of the helix. In this case, irrespective of the initial helix geometry or amplitude of displacements, these equations admit complete and general, traveling-wave, analytical solutions as periodic or solitary waves which possess axial and angular momenta. [1]

In [2], Eqs. (1) and (2) were resolved analytically for the particular case of a solitary wave in a helix which is stationary at infinity. In the solution, the constants of integration were chosen appropriately to maintain the initial shape of the helix at infinity in front of the wave. We now remove this requirement and construct the general traveling

* Corresponding author. E-mail: vadis@eng.tau.ac.il.

[1] These waves are stationary in a coordinate system uniformly moving along and rotating around the helix axis.

PII S0165-2125(97)00045-0

wave solution which describes both a periodic wave as well as a solitary wave. Moreover, in the case of the solitary wave, the more general condition at infinity includes possible rigid body rotation of the helix.

Since there exists no strain energy in the system under consideration, geometrical nonlinearity is essential for the wave phenomena. Waveguides in which geometrical nonlinearity is significant were considered in a number of works. Gorbacheva and Ostrovsky [3] investigated plane transverse motions of an initially straight atomic chain (a mass-spring system). Spatial solitary waves in similar systems were considered by Cadet [4] and Rosenau [5]. There is a large body of works devoted to the nonlinear dynamics of inextensible fibers and elastic strings. As a result of mathematical difficulties, most of them are based on approximate methods to take into account the coupled transversal and longitudinal motions. The study of the dynamic behavior of fibers based on genuinely nonlinear Eq. (1) was started by Kolodner [6] and continued by many authors (note works by Reeken [7] and Antman and Reeken [8]). The equation for the large vibration of strings was studied in [9–11]. Some solutions of Eq. (1) were found by Rosenau and Rubin [12] for an extensible fiber in the cases of the time-independent and coordinate-independent tension. For an extended reference and historical notes see, for example, the book by Antman [13]. Solitary waves in an extensible string of an arbitrary nonlinear elastic material were described in [14]. It was shown that neglecting extensibility leads to a low-velocity asymptote (or low-energy) of the solution for the corresponding extensible fiber. Different types of solitary waves in the helical string rotating as a rigid body were later considered in [15].

It may be mentioned that the model of the inextensible flexible helical fiber is relevant to a wide variety of fields: from the modeling of macromolecules such as DNA to reinforcements of composite materials, textile yarn manufacturing processes, modeling of mechanical properties of helical strands [16] and deployable antennae for satellite applications [17]. Moreover, such systems can be used as an energy absorber under dynamic extension [18]. Note that the deployable systems may also serve as demonstrations of the solitary waves. The helical inextensible fiber devoid of bending stiffness, considered in the present work, is the simplest system of this kind. Such a model corresponds to a long-wave approximation, where the radius of curvature of the fiber as well as the wave length is much larger than the cross-sectional dimensions of the fiber.

In addition to [2], some results related to the present problem were presented in the works by the authors [19–21].

We represent the position vector $\mathcal{R}(S,t)$ as the sum of a longitudinal vector $\boldsymbol{R}_x(S,t)$, where x is the axis of the helix (associated with the unit vector $\boldsymbol{k}_x$) and a vector $\boldsymbol{R}(S,t)$ lying in the cross-section of the helix [2]. Introducing the nondimensional quantities

$$\boldsymbol{r}_x = \boldsymbol{R}_x/R_0, \quad \boldsymbol{r} = \boldsymbol{R}/R_0, \quad s = S/R_0, \quad f = F/\rho v^2, \quad \tau = vt/R_0, \tag{3}$$

where v is the wave velocity along the fiber, and R_0 is the radius of the undeformed helix, the vectors $\boldsymbol{r}_x$ and $\boldsymbol{r}$ are represented as follows (Fig. 1):

$$\boldsymbol{r}_x(s,\tau) = r_x(s,\tau)\boldsymbol{k}_x = [s\cos\gamma + u(\xi)]\boldsymbol{k}_x, \qquad \boldsymbol{r}(s,\tau) = A(\xi)\,\mathrm{e}^{\mathrm{i}\lambda s + \mathrm{i}\omega\tau}, \tag{4a,b}$$

$$\lambda = \sin\gamma, \qquad \xi = s - \tau. \tag{4c,d}$$

Here $\gamma \in (0, \pi/2]$ is the angle between the fiber and the x-axis in the undeformed helix; ω is a real parameter relating to the angular velocity of the helix; $A(\xi)$ and $u(\xi)$ are unspecified functions. The rotating vector $\boldsymbol{r}(s,\xi)$ is defined in a complex variable plane which coincides with the cross-section of the helix, and $A(\xi)$ is a complex function.[2] Note that the complex representation of the rotating vector $\boldsymbol{r}$, Eq. (4b), was shown in [5] to permit a traveling wave solution for the corresponding plane problem, i.e. an infinite 'helix' with zero pitch.

[2] The representation (4) differs from that in [2] by the parameter ω which is introduced in Eq. (4b) to take explicitly into account the possibility of rotation of the helix as a rigid body. This representation corresponds physically to an observer attached to an orthogonal right-hand triad natural to the undeformed helix which moves along the fiber with a speed v and an associated angular velocity Ω about the x-axis, $\Omega = (\lambda + \omega)v/R_0$.

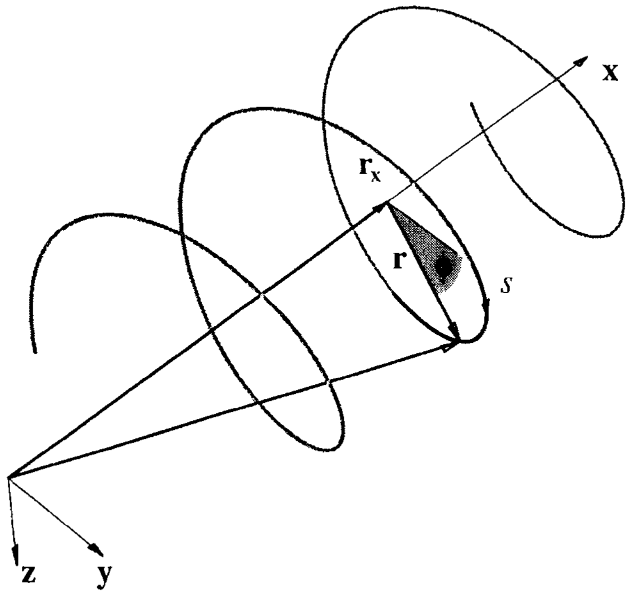

Fig. 1. Representation of the position vector.

Substituting (4) into Eq. (1) then leads to

$$[(\cos\gamma + u')f]' = u'', \quad (1-f)\boldsymbol{r}'' - f'r' - \sigma^2 \boldsymbol{r} - 2\mathrm{i}\sigma \boldsymbol{r}' = 0, \tag{5a,b}$$

with the inextensibility condition

$$|\boldsymbol{r}'|^2 + |\boldsymbol{r}_x'|^2 = 1. \tag{5c}$$

Here and below, $\sigma = \lambda + \omega$; primes and dots denote derivatives with respect to the nondimensional coordinate, s and time τ, respectively.

Integration of the system (5) with four unknowns, $u(\xi)$, $f(\xi)$, $|\boldsymbol{r}(\xi)|$ and $\arg[\boldsymbol{r}(\xi)]$, yields a general solution which involves seven scalar constants of integration. Using the same integration procedure as was applied in [2], we obtain sequentially the following relations: the expression for u' follows from Eq. (5a); namely

$$u' = -\cos\gamma + \frac{C_1}{1-f}, \tag{6}$$

where C_1 is a constant of integration. From inextensibility condition (5c), we have the expression

$$|\boldsymbol{r}'|^2 = 1 - |\boldsymbol{r}_x'|^2 = 1 - \frac{C_1^2}{(1-f)^2}, \tag{7}$$

which, together with Eq. (5b), yields the relation between the nondimensional tension force, f, and the helix radius, $|\boldsymbol{r}(s,\tau)|$:

$$f' = -\tfrac{1}{2}\sigma^2(|\boldsymbol{r}|^2)', \qquad f = \tfrac{1}{2}\sigma^2(C_2 - |\boldsymbol{r}|^2) \qquad (\lambda \neq -\omega), \tag{8a,b}$$

where $C_2 > 0$ is a constant of integration. Note that the constant C_1 does not appear in this relation but appears only in the expression for u'.

It follows from Eq. (5b) that the case $\sigma = 0, \boldsymbol{r}' \neq \text{const}$[3] corresponds to the D'Alembert solution $\mathcal{R} = \mathcal{R}(S - vt)$, $f = 1$, described in [2], as a uniform flow of the fiber material along an arbitrary curve under the condition of a constant internal force.[4] Hereafter the parameter σ is taken to be nonzero.

Substituting Eq. (8b) back into Eq. (5b) and rearranging leads to

$$\boldsymbol{r}'' - \tfrac{1}{2}\sigma^2 [(C_2 - |\boldsymbol{r}|^2)\boldsymbol{r}']' - \sigma^2 \boldsymbol{r} - 2\mathrm{i}\sigma \boldsymbol{r}' = 0. \tag{9}$$

In solving this 2D vector equation, we choose to represent the vector $\boldsymbol{r}$ by means of the specific complex representation

$$A(\xi) = r(\xi)\mathrm{e}^{\mathrm{i}\theta(\xi)}, \qquad \boldsymbol{r} = r(\xi)\mathrm{e}^{\mathrm{i}\phi(s,\tau)}, \qquad \phi(\xi, s) = \theta(\xi) + \lambda s + \omega\tau, \tag{10a,b,c}$$

where $r(\xi)$ and $\theta(\xi)$ are real functions. Substituting Eq. (10) into Eq. (9) and separating the real and imaginary parts, we obtain the equations

$$[1 - \tfrac{1}{2}\sigma^2(C_2 - r^2)][r'' - (\phi')^2 r] + \sigma^2 r (r')^2 - \sigma^2 r + 2\sigma\phi' r = 0, \tag{11a}$$

$$[1 - \tfrac{1}{2}\sigma^2(C_2 - r^2)](\phi'' r + 2\phi' r') + \sigma^2 r^2 r' \phi' - 2\sigma r' = 0, \tag{11b}$$

which, together with expression (8b), govern the traveling waves in the helix.

In Section 2, the general traveling-wave solution which contains seven arbitrary, scalar constants of integration is derived . In Sections 3 and 4, we analyze two different types of waves: the first corresponds to the case when the fiber crosses the axis of the helix; in the second, the fiber does not cross the axis. Integral properties of the solution are considered in Section 5.

2. General traveling-wave solution

When the initial shape of the helix remains constant ($r' = 0$, $\phi' = \lambda$, $r \neq 0$), Eq. (11b) is satisfied automatically and Eq. (11a), which takes the form

$$\lambda^2 f - \omega^2 = 0, \tag{11c}$$

describes the rotation of the undeformed helix with the nondimensional angular velocity $\omega = \pm\lambda\sqrt{f}$. However, Eqs. (11a,b) also lead to some wave solutions. To this end, we first consider Eq. (11b) which is linear and of first order in ϕ'. Eq. (11b) admits the solution

$$\phi' = \frac{\sigma}{1 - f} + \frac{\sigma^2 C_3}{2r^2(1 - f)}, \tag{12a}$$

$$\theta' = \phi' - \lambda = \frac{\lambda f + \omega}{1 - f} + \frac{\sigma^2 C_3}{2r^2(1 - f)}, \tag{12b}$$

where $C_3 = \text{const}$, and f is defined by Eq. (8b). Substitution of expression (12a) into Eq. (11a) yields a second-order equation with respect to r; namely

$$r'' + \sigma^2 r \frac{(r')^2 - 1}{1 - (\sigma^2/2)(C_2 - r^2)} + \sigma^2 r \frac{1}{[1 - (\sigma^2/2)(C_2 - r^2)]^2} - \frac{\sigma^4 C_3^2}{4r^3[1 - (\sigma^2/2)(C_2 - r^2)]^2} = 0. \tag{13}$$

[3] The case $\boldsymbol{r}' = \text{const}$ corresponds to a rectilinear fiber which, being inextensible, cannot be a waveguide.

[4] The rotation of the helix as a rigid body with the nondimensional angular velocity $\omega = -\lambda$ corresponds to this solution since the constant axial velocity, $v_x = -v\cos\gamma$, can always be added.

This equation can be rewritten as a first-order equation with respect to $(r')^2 - 1$ whose solution includes the next constant of integration, C_4:

$$r' = \pm\frac{\sigma^2}{2}\frac{\sqrt{r^2(C_2 - r^2)^2 - r^2C_4 - C_3^2}}{r\,[1 - (\sigma^2/2)(C_2 - r^2)]}. \tag{14}$$

The choice of the sign in Eq. (14) is discussed below where the solutions for zero and nonzero minimal values of r^2 are considered. Before integrating this equation, we first consider some relations concerned with the determination of the constants. From representation (10), it follows that

$$|\boldsymbol{r}'|^2 = (r')^2 + r^2(\phi')^2, \tag{15}$$

and Eqs. (12a) and (14) yield

$$|\boldsymbol{r}'|^2 = 1 - \frac{1 - \sigma^2C_2 + \sigma^4/4\,C_4 - \sigma^3\,C_3}{(1-f)^2}. \tag{16}$$

On the other hand, noting that $|\boldsymbol{r}'|^2$ is defined by Eq. (7), we find the expression for C_1, namely

$$C_1 = \pm\sqrt{1 - \sigma^2C_2 + (\sigma^4/4)C_4 - \sigma^3\,C_3}. \tag{17}$$

Since the constant C_1 is real (see Eq. (6)),

$$C_1^2 \geq 0. \tag{18a}$$

Then from the inextensibility condition, Eq. (5c), we have $|\boldsymbol{r}'|^2 \leq 1$, and therefore, from Eq. (7)

$$\frac{C_1^2}{(1-f)^2} \leq 1. \tag{18b}$$

Further, from Eqs. (6) and (18b), it follows that $-(1+\cos\gamma) \leq u' \leq 1 - \cos\gamma$. The choice of the sign in Eq. (17) has a geometrical meaning and depends on the correspondence of the positive directions of the coordinates s and x. Note that if x increases with s, $r_x' = C_1/(1-f) \geq 0$. Hereafter, we assume that $r_x' \geq 0$ and, consequently, $\mathrm{sgn}(C_1) = \mathrm{sgn}(1-f)$.

We observe that in the case of the equality in (18b), $|\boldsymbol{r}'| = 0$ (see Eq. (7)). In this case, $|\boldsymbol{r}_x'(\xi)| = 1$ and the helix degenerates to a straight line. In the other limiting case when $C_1 = 0$, we have $\boldsymbol{r}_x'(\xi) = 0$ and $|\boldsymbol{r}'| = 1$ for all ξ. Physically this corresponds to the fiber as a plane curve with x =const.

Now integrating differential equations (14), (6) and (12a), and noting that for the functions $r(\xi)$, $u(\xi)$ and $\theta(\xi)$, the equalities are valid as $\partial/\partial s = \partial/\partial\xi = (\partial/\partial r)(\mathrm{d}r/\mathrm{d}\xi)$, we obtain the general solution of the system (Eq. (5)) in a form which is valid for any interval where $\xi(r)$ is a single-valued function:

$$\xi(r) = \pm\frac{2}{\sigma^2}\int_{r_0}^{r}\frac{1 - (\sigma^2/2)(C_2 - r^2)}{\sqrt{r^2(C_2 - r^2)^2 - r^2\,C_4 - C_3^2}}\,r\,\mathrm{d}r + C_5, \tag{19a}$$

$$u(\xi) = -\xi\cos\gamma \pm \frac{2}{\sigma^2}\int_{r_0}^{r}\frac{C_1}{\sqrt{r^2(C_2 - r^2)^2 - r^2\,C_4 - C_3^2}}\,r\,\mathrm{d}r + C_6, \tag{19b}$$

$$\theta(\xi) = \pm\int_{r_0}^{r}\frac{\sigma\,r^2\,(C_2 - r^2) + C_3}{\sqrt{r^2(C_2 - r^2)^2 - r^2\,C_4 - C_3^2}}\,\frac{\mathrm{d}r}{r} + C_7, \tag{19c}$$

or, alternatively

$$\theta(\xi) = \pm\frac{1}{\sigma}\int\limits_{r_0}^{r}\frac{2r^2+\sigma C_3}{\sqrt{r^2(C_2-r^2)^2-r^2 C_4-C_3^2}}\frac{\mathrm{d}r}{r}-\lambda\xi+C_7, \tag{19d}$$

where r_0 is the minimal nonnegative value of r; the internal force $f(r)$ is defined by Eq. (8) and the angle $\phi(s,\tau)$ can be obtained using Eq. (10c). We observe that the constants C_6 and C_7 correspond respectively to the axial displacement and rotation of the helix as a rigid body and hence are not essential for our consideration. Nevertheless we save these constants in order to satisfy the conditions of the undeformed helix at infinity in front of the solitary wave. Letting the constant $C_5 = \xi(r_0)$ correspond to the origin of the ξ-coordinate position, we choose the coordinate system such that $C_5 = 0$ and $r = r_0(\xi = 0)$. In effect, the resulting solution then depends on the three scalar constants C_2, C_3, C_4 and also on the parameter σ. Our goal is to analyze this general solution for any possible combination of the constants.

With this in mind, it is convenient to separate the solutions into two types: the first one, $r_0 = 0$, corresponds to the case where the fiber crosses the x-axis at the point $\xi = 0$, and the second type corresponds to a nonzero minimal radius of the deformed helix.

3. The case $r_0 = 0$ (the fiber crosses the axis of the helix)

3.1. General description

Noting, that r' and ϕ' have been introduced as real values, it follows from Eq. (12) that C_3 is real. Further, it follows from Eq. (14) that r' would be imaginary for small r if $C_3 \neq 0$. Hence solutions for which $r_0 = 0$ are described by Eq. (19a,b,c) under the condition $C_3 = 0$. (Moreover, one observes that in the case, $r_0 = 0$, the integrand in Eq. (19c) is nonintegrable if $C_3 \neq 0$.)

It follows from (14) that at the point $r = \xi = 0$, the derivative r' has a nonzero value if $C_2^2 \neq C_4$:

$$[r'(0)]^2 = \frac{\sigma^4}{4}\frac{C_2^2-C_4}{[1-(\sigma^2/2)C_2]^2}. \tag{20}$$

Thus, in this case, the fiber crosses the axis of the helix at the point $\xi = 0$. (The case $C_2^2 = C_4$ is considered below.) We find it convenient to define $r = |\boldsymbol{r}|$for $\xi \geq 0$ and $r = -|\boldsymbol{r}|$ for $\xi \leq 0$. As a result of this definition, we take the sign "+" in Eqs. (14) and (19) for $f < 1$ and the sign "–" for $f > 1$. In accordance with Eqs. (14), (17), (8b) and (6), we obtain

$$r' = \pm\frac{\sigma^2}{2}\frac{\sqrt{(C_2-r^2)^2-C_4}}{1-(\sigma^2/2)(C_2-r^2)} = \frac{\sigma^2}{2}\frac{\sqrt{(C_2-r^2)^2-C_4}}{|1-f|}, \tag{21}$$

$$u'(r) = -\cos\gamma + \frac{\sqrt{1-\sigma^2 C_2+(\sigma^4/4)C_4}}{1-f}. \tag{22}$$

Taking into account Eqs. (20) and (21) one has

$$C_2^2 \geq C_4, \qquad (C_2-r^2)^2-C_4 \geq 0. \tag{23a,b}$$

For $C_3 = 0$, expression (19a) can then be reduced to the form

$$\frac{\sigma^2}{2}\xi = \pm\int\limits_0^r \frac{1-(\sigma^2/2)(C_2-r^2)}{\sqrt{(r_1^2-r^2)(r_2^2-r^2)}}\,\mathrm{d}r, \tag{24}$$

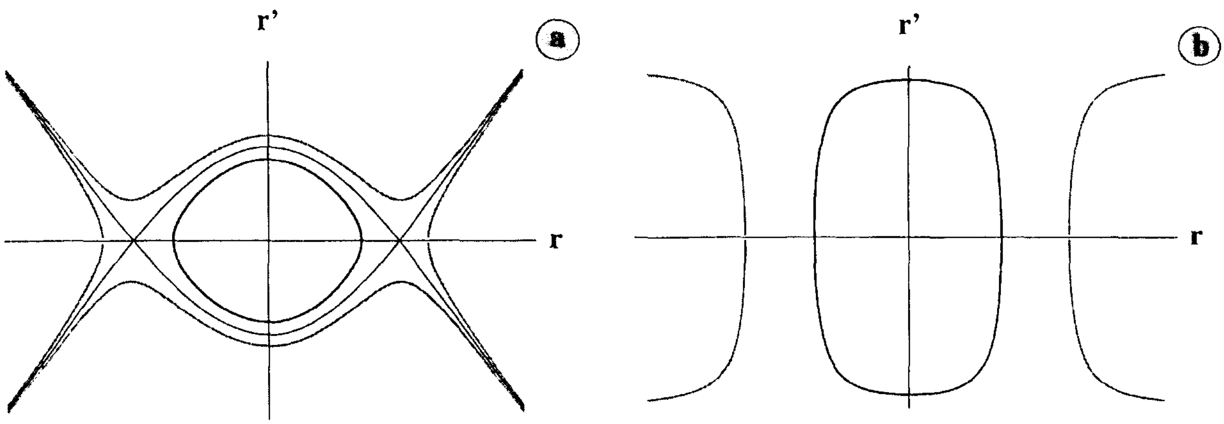

Fig. 2. Phase portrait for Eq. (13) with $C_3 = 0$: (a) $f < 1$; (b) $f > 1$. Observe that this phase portrait is similar in appearance to that of a non-linear oscillator.

where

$$r_1^2 = C_2 + \sqrt{C_4}, \qquad r_2^2 = C_2 - \sqrt{C_4} \tag{25a,b}$$

are the roots of the equation

$$(C_2 - r^2)^2 - C_4 = 0. \tag{25c}$$

The phase portrait of Eq. (14) with $C_3 = 0$ is shown in Figs. 2(a) and (b). We observe that the ordinary differential equation (13) leads to periodic waves, solitary waves and increasing solutions corresponding to $C_4 > 0$, $C_4 = 0$ and $C_4 < 0$ respectively.[5] The case $C_4 < 0$ corresponds physically to a negative tension force and we exclude it from consideration. From the inextensibility condition and from Eq. (21), it follows that the solitary wave solution ($C_4 = 0$) satisfies the following condition:

$$\frac{f}{|1-f|} \le 1; \qquad f \le \frac{1}{2}. \tag{26}$$

Finally, if $C_4 > 0$, Eq. (25c) has two real roots, and the expression under the square root in Eq. (21) is nonnegative in the relevant ranges $0 \le r \le r_2$ and $r_1 \le r \le \infty$. We exclude the case $r \ge r_1$ from our consideration below since it corresponds to an unbounded solution with a negative internal force. We therefore need consider only the remaining relevant case, $C_4 > 0$, $0 \le r \le r_2$.

3.2. Periodic wave

In this case, the phase curve is closed; it corresponds to a periodic solution (see Figs. 2(a) and (b)), which can be expressed in terms of elliptic integrals. The relations between r and ξ follow from Eq. (24) as

$$r_1 \frac{\sigma^2}{2} \xi = \pm \left[1 - \frac{\sigma^2}{2} (C_2 - r_1^2) \right] \mathrm{F}(\varphi, k) \mp \frac{\sigma^2}{2} r_1^2 \mathrm{E}(\varphi, k), \tag{27}$$

[5] Note, however, that Eq. (1) is a vector equation, and r is a scalar. Therefore the phase portrait of Eq. (13) does not give the complete description of the movement of the system.

from which

$$r = \pm r_2 \operatorname{sn}\left[r_1 \frac{\sigma^2}{2} \frac{\xi \pm r_1 \mathrm{E}(\varphi, k)}{1 + (\lambda^2/2)\sqrt{C_4}} \right], \tag{28}$$

where

$$\mathrm{F}(\varphi, k) = \int_0^{\varphi} \frac{\mathrm{d}\varphi}{\sqrt{1 - k^2 \sin^2 \varphi}}, \qquad \boldsymbol{K}(k) = \int_0^{\pi/2} \frac{\mathrm{d}\varphi}{\sqrt{1 - k^2 \sin^2 \varphi}},$$

$$\mathrm{E}(\varphi, k) = \int_0^{\varphi} \sqrt{1 - k^2 \sin^2 \varphi}\, \mathrm{d}\varphi, \qquad \boldsymbol{E}(k) = \int_0^{\pi/2} \sqrt{1 - k^2 \sin^2 \varphi}\, \mathrm{d}\varphi.$$

Here $\mathrm{F}(\varphi, k)$ and $\mathrm{E}(\varphi, k)$ are elliptic integrals in Legendre's normal form of the first and the second kind, respectively; sn is Jacobi's elliptic sine; $k = r_2/r_1 \leq 1$ and $\varphi = \arcsin(r/r_2)$ are, respectively, the modulus and the argument of the elliptic integrals.

It follows from expressions (8b) and (25) that the constants C_2 and $\sqrt{C_4}$ correspond, respectively, to maximum and minimum values of the internal force, f; namely

$$f = f_{\min} = \frac{\sigma^2}{2} \sqrt{C_4} \quad (r = r_2), \qquad f = f_{\max} = \frac{\sigma^2}{2} C_2 \quad (r = 0). \tag{29}$$

In the limiting case $C_2^2 = C_4$, we note that for $f > 0$, r' is real only if $r = 0$ for all ξ and hence the helix degenerates to a straight fiber.

Having obtained relation (8b) between r and f, the solution (28) can be rewritten alternatively in terms of the internal force. Taking the square of both parts of Eq. (28), adding $-C_2$ and multiplying by $\sigma^2/2$ we obtain

$$\eta = \eta_{\max} \operatorname{cn}^2 \left[\sqrt{f_{\min} + \eta_{\max}/2}\; \frac{|\sigma|\xi \pm 2\sqrt{f_{\min} + \eta_{\max}/2}\, \mathrm{E}(\varphi, k)}{1 + f_{\min}} \right], \tag{30}$$

where $\eta \equiv f - f_{\min}$ is the current amplitude of the wave, $\eta_{\max} \equiv f_{\max} - f_{\min}$ is the maximal amplitude and cn denotes Jacobi's elliptic cosine.

Let L be the wave length, i.e. $r(\xi) = r(\xi + L)$. We observe that the functions $r'(r)$, $\phi'(r)$, $u'(r)$ and $f(r)$ are also periodic since they depend only on r. Noting that the period of the elliptic function is $4\boldsymbol{K}(k)$ and that of the square of the elliptic function is $2\boldsymbol{K}(k)$, Eq. (30) yields a relation for the wave length:

$$r_1 \frac{\sigma^2}{2} \frac{L}{2} = \pm \left[1 - \frac{\sigma^2}{2} (C_2 - r_1^2) \right] \boldsymbol{K}(k) \mp \frac{\sigma^2}{2} r_1^2 \boldsymbol{E}(k), \tag{31a}$$

which, using Eqs. (25) and (29), can be expressed as

$$\frac{|\sigma|}{\sqrt{2}} \frac{L}{2} = \pm \frac{1 + f_{\min}}{\sqrt{f_{\min} + f_{\max}}} \boldsymbol{K}(k) \mp \sqrt{f_{\min} + f_{\max}}\, \boldsymbol{E}(k). \tag{31b}$$

Thus, we have obtained a two-parameter set of solutions (noting that the three parameters, $f_{\max}$, $f_{\min}$ and the wave length L, are connected by Eq. (31b)).

Having set $C_3 = 0$ (since the case $r_0 = 0$ is under consideration) and using Eqs. (19b,c), we obtain expressions for the axial displacement and angle of rotation:

$$u(\xi) = -\xi \cos\gamma + \frac{\sqrt{2}}{|\sigma|} \frac{\sqrt{1 - 2f_{\max} + f_{\min}^2}}{\sqrt{f_{\min} + f_{\max}}} \mathrm{F}(\varphi, k) + C_6, \tag{32}$$

$$\theta(\xi) = \pm\frac{\sqrt{2}}{\sqrt{f_{\min} + f_{\max}}}\,\mathrm{F}(\varphi, k) - \lambda\xi + C_7, \tag{33a}$$

$$\phi(s, \tau) = \theta(\xi) + \lambda s + \omega\tau = \pm\frac{\sqrt{2}}{\sqrt{f_{\max} + f_{\min}}}\mathrm{F}(\varphi, k) + \sigma\tau. \tag{33b}$$

Note that the axial displacement $u(\xi, r)$ as well as the angle of rotation $\theta(\xi, r)$ can be expressed as a sum of periodic and linear functions of ξ. This means that each passing wave leads to a constant shift in the axial displacement and rotation and gives rise to constant components of the linear and angular velocities.

We can now draw some conclusions concerning the limits of the internal force. From expression (32) we observe that the limits, $f_{\min}$ and $f_{\max}$, cannot be chosen arbitrarily since these values must satisfy the inequality

$$f_{\max} \le \tfrac{1}{2}(1 + f_{\min}^2) \quad \text{or} \quad f_{\max} - f_{\min} \le \tfrac{1}{2}(1 - f_{\min})^2. \tag{34a,b}$$

Hence, any one of the following relations can be valid:

$$f_{\min} < f_{\max} < 1, \qquad 1 < f_{\min} < f_{\max}, \qquad f_{\min} = f_{\max} = 1. \tag{34c,d,e}$$

In the latter, degenerate case, the internal force is invariable: $f \equiv 1$, and it is not a wave solution. Upon setting $f_{\min}^2 = a f_{\max}^2$, where $0 \le a \le 1$, we then have the following sub-classes of the solution:

$$f_{\min} = \frac{1}{\sqrt{a}}(1 - \sqrt{1-a}) \le f \le \frac{1}{a}(1 - \sqrt{1-a}) = f_{\max} = f_{\max}^{(1)} \quad (f_{\max}^{(1)} \le 1), \tag{35a}$$

$$f_{\min}^{(2)} = f_{\min} = \frac{1}{\sqrt{a}}(1 + \sqrt{1-a}) \le f \le \frac{1}{a}(1 + \sqrt{1-a}) = f_{\max} \quad (f_{\min}^{(2)} \ge 1), \tag{35b}$$

where $f_{\max}^{(1)}$ and $f_{\min}^{(2)}$ correspond to the equalities in Eqs. (34a,b).

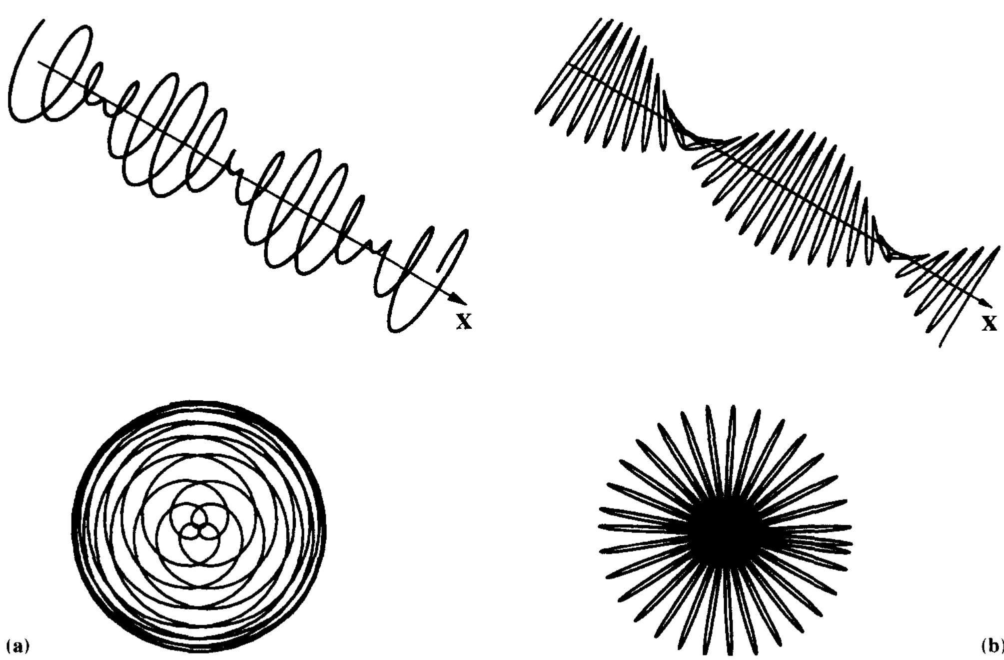

Fig. 3. Shape of the deformed helix with $r_0 = 0$ at any given time for $\sigma = \sin(\pi/18)$, $a = 0.25$: (a) $f < 1$, $f_{\max} = \sigma^2/2$; (b) $f > 1$, $f_{\max} = 200 f_{\max}^{(2)}$. The fiber is shown compressed along the x-axis. The lower picture represents the shape of the fiber viewed from a point lying on the x-axis.

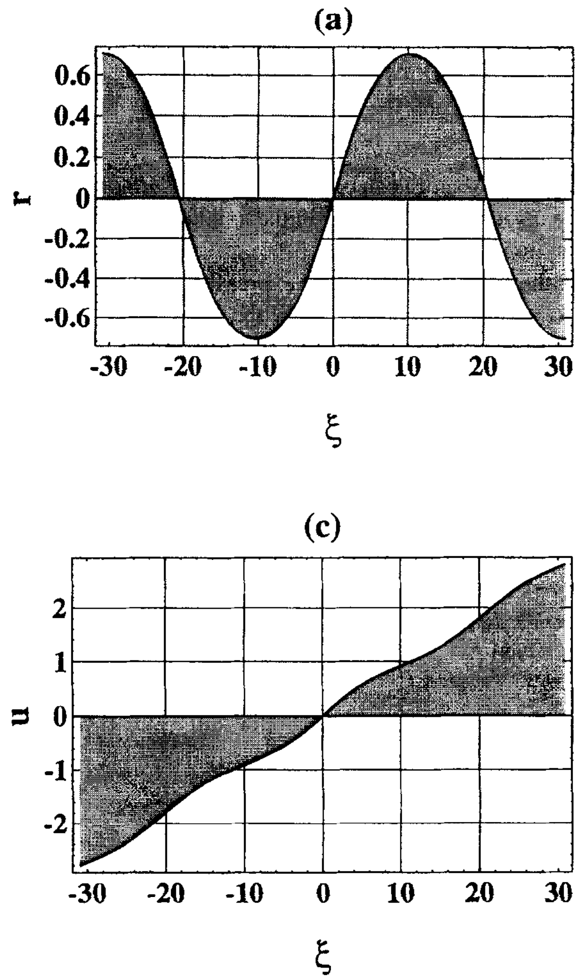

Fig. 4. Components of the periodic solution for $r_0 = 0$: (a) radius of the helix $r(\xi)$; (b) internal force $f(\xi)$; (c) axial displacement $u(\xi)$; (d) angle of rotation $\theta(\xi)$.

The deformed shape of a helix with $\gamma = \pi/18$, $a = 0.25$ due to a propagating periodic wave is presented in Figs. 3(a) and (b) for the cases $f < 1$ and $f > 1$, respectively. We observe that for $f < 1$, $\phi_+ - \phi_- > \pi/2$ where ϕ_+ and ϕ_- correspond to the maximal and minimal values of r respectively; for the case $f > 1$, $\phi_+ - \phi_- < \pi/2$.

Figures of $r(\xi)$, $f(\xi)$, $u(\xi)$ and $\theta(\xi)$ are shown in Figs. 4 (a)–(d), respectively, for values $C_2 = 1$, $a = 0.25$ and $\gamma = \pi/6$.

3.3. Solitary wave

We first observe that the wave length, given by Eq. (31b), depends on the ratio $k = r_2/r_1$ and hence, via Eq. (25a,b), on the constant C_4. The limiting case, $C_4 = 0$, corresponds to the infinite wavelength, $L = \infty$. In this case, as follows from Eqs. (8b), (25), (26), (29) and (34),

$$r_1 = r_2 = C_2, \quad k = 1, \quad f_{\min} = 0, \quad f_{\max} = \tfrac{1}{2}\sigma^2 C_2 \le \tfrac{1}{2}. \tag{36a–d}$$

Keeping the definition $|\mathbf{R}| = R_0$ and $\theta = 0$ for the undeformed helix, $\xi = +\infty$, we find $C_2 = 1$, $\omega = 0$ ($\theta = \lambda$), $C_7 = -\lambda$. Then, setting $C_6 = -\cos\gamma$ we also obtain the required equality, $u = 0$ for the axial displacement at $\xi = +\infty$. As a result, we have the relations which describe a solitary wave:

$$r = \tanh\left[\frac{\lambda^2}{2}(\xi + r)\right], \qquad u = (r-1)\cos\gamma, \tag{37a,b}$$

$$\theta = \lambda(r-1), \qquad f = \frac{\lambda^2}{2}(1-r^2) = \frac{\lambda^2}{2}\,\mathrm{sech}^2\left[\frac{\lambda^2}{2}(\xi + r)\right]. \tag{37c,d}$$

This solution reveals that the effective wavelength is independent of the amplitude (and velocity) and depends only on the parameter λ [2,20]. Note that this result is a consequence of the inextensibility of the fiber. As is shown in [14], the model of an inextensible fiber is the low-velocity asymptote of an elastic string (the wave velocity is far less then the local sound velocity in the string material). In this case, the geometrical nonlinearity due to the flexibility of the fiber plays a decisive role in the formation of the wave.

We also note from the above derived solution, that in the case of rigid body rotation of the helix, solitary waves do not exist for cases in which the fiber crosses the helix axis.

3.4. Asymptotic solutions

It was shown in [20] that in the case $\lambda \to 0$, Eqs. (36) and (37) yield the asymptotic expression $f \sim (\lambda^2/2)\,\mathrm{sech}^2[(\lambda^2/2)\xi]$. Here we consider an asymptotic solution which corresponds to a periodic wave of a small amplitude of the force variation: $\eta_{max}/f_{max} \equiv \varepsilon \ll 1$. Note that this condition is the same as $\lambda \to 0$ since the limit, $\varepsilon = 0$, corresponds to the straight fiber. Noting that $r_2 \sim \sqrt{C_2\varepsilon}$, for small ε we have $r_1 \sim \sqrt{2C_2}$, $k \sim \sqrt{\varepsilon/2}$, $\mathrm{F}(\varphi, k) = \mathrm{E}(\varphi, k) \sim \arcsin(r/r_2)$; the solution can then be expressed in terms of trigonometric functions:

$$r(\xi) \sim \pm r_2 \sin\left(\frac{q}{2}\xi\right), \qquad \eta(\xi) \sim \frac{\eta_{max}}{2} + \frac{\eta_{max}}{2}\cos(q\,\xi), \tag{38a,b}$$

where

$$q = 2\sqrt{f_{max}}\left|\frac{\sigma}{1 - f_{max}}\right|, \tag{39a}$$

or, in dimensional form (see Eq. (3)),

$$\frac{q}{R_0} = 2v\sqrt{\rho F_{max}}\left|\frac{\sigma}{\rho v^2 - F_{max}}\right|. \tag{39b}$$

For this sinusoidal wave, Eq. (39) yields the dispersion relation where q/R_0 corresponds to a wave number [22]. Note that the amplitude η_{max} of the force does not appear in the dispersion relation. From Eq. (34b,c), it follows that $f_{max} \le 1 - \sqrt{2\varepsilon}$ or $f_{max} \ge 1 + \sqrt{2\varepsilon}$ and hence $q \le 2\,|\sigma|/\sqrt{2\,\varepsilon}$.

4. The case $r_0 \neq 0$ (the fiber does not cross the axis of the helix)

4.1. General considerations

In this case, the solution is described by Eqs. (8) and (19) with $C_3 \neq 0$. The solution exists when the expression under the square root in Eq. (14) is positive; hence the type of solution is defined by the character of the roots of the equation below, hereafter denoted by $r_3^2 \le r_2^2 \le r_1^2$,

$$r^6 - 2C_2r^4 + (C_2^2 - C_4)r^2 - C_3^2 = 0, \tag{40a}$$

which can be written in the form

$$\beta(1-\beta)^2 = a\beta + b^2, \tag{40b}$$

where

$$\beta = r^2/C_2, \qquad a = C_4/C_2^2, \qquad b = C_3/C_2^{3/2}. \tag{40c}$$

The roots r_3 and r_2, if they exist, define the boundaries of the range where the left-hand part of Eq. (40a) is positive, and correspond to the minimal and maximal radii, respectively. The left-hand side of Eq. (40b), with roots $\beta = 0$ and $\beta = 1$, does not depend on the constants a and b, while the right-hand side is the straight line. We note that the roots of Eq. (40a,b) do not depend on the sign of C_3 which in principle can be negative. Note also that the periodic solution may be obtained both for $C_4 > 0$ and for $C_4 < 0$ for $C_3 \neq 0$ (as noted in Section 4.1, if $C_3 = 0$ the bounded solution exists only for $C_4 \geq 0$). The solitary wave solution exists only for $C_4 < 0$. The phase portrait for the case $f < 1$ is shown in Fig. 5(a), and for the case $f > 1$ in Fig. 5(b).

Similarly, as in the case $C_3 = 0$, the constants C_2, C_3, C_4 cannot be prescribed arbitrarily but must satisfy conditions (18a,b). Condition (18b) is satisfied automatically if $r_3 < r < r_2$. From condition (18a), we have, using the notations of Eq. (40c):

$$a\alpha^4 - 2\alpha^2 + 1 = \mathrm{sgn}(\sigma C_3)\sqrt{8}|b|\alpha^3, \qquad \alpha = \sqrt{(\sigma^2/2)C_2}. \tag{41a,b}$$

Eq. (41a) has one or two positive roots, $\alpha^{(1)}$ and $\alpha^{(2)}$. The number of roots depends on the relationship between the parameters a, b and the sign of the product σC_3. In the case $a \leq 0$, only one positive root exists. In the case $a > 0$, Eq. (41a) has two positive roots and the internal force can be unbounded. The possible combinations are shown on Fig. 6. From Eqs. (41a,b) and (8b), we obtain the limiting values of the internal force:

$$f_{\max}^{(1)}[a, b, \mathrm{sgn}(\sigma C_3)] = \alpha^{(1)}[a, b, \mathrm{sgn}(\sigma C_3)][1 - \beta_3(a, b)], \tag{42a}$$

$$f_{\min}^{(2)}[a, b, \mathrm{sgn}(\sigma C_3)] = \alpha^{(2)}[a, b, \mathrm{sgn}(\sigma C_3)][1 - \beta_2(a, b)]. \tag{42b}$$

Thus, the internal force must satisfy condition (35a) or (35b) according to the number of roots of Eq. (41a). Note that in the case of the solitary wave, when $a < 0$, Eq. (41a) has only one positive root and $\alpha^{(1)} < 1$ (see Fig. 6); therefore, in this case, $f < 1$. As noted above, when the force takes the limiting values (42a,b), the helix degenerates to a plane curve.

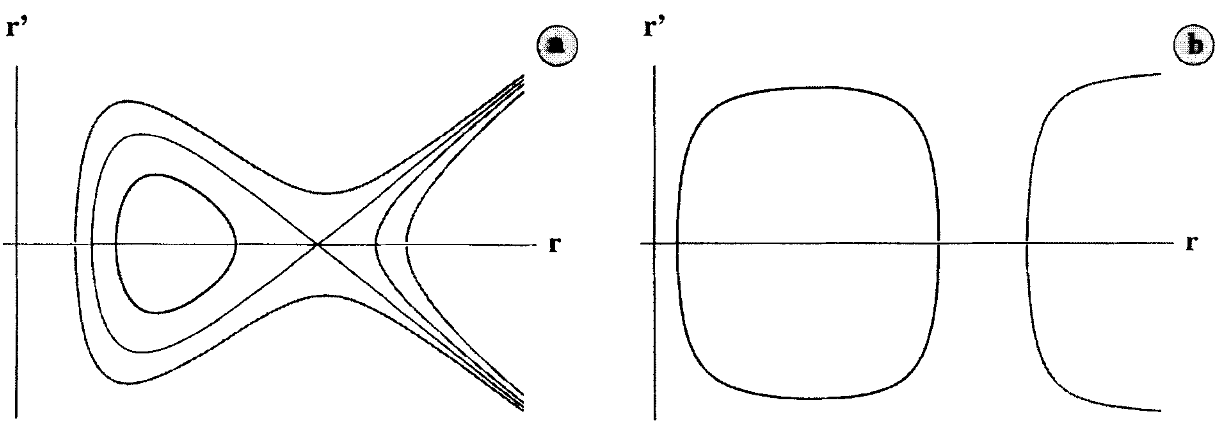

Fig. 5. Phase portrait for Eq. (13) with $C_3 \neq 0$: (a) $f < 1$; the separatrix corresponds to the solitary wave solution, and the closed curves correspond to periodic solution; (b) $f > 1$; observe that only a periodic wave solution exists.

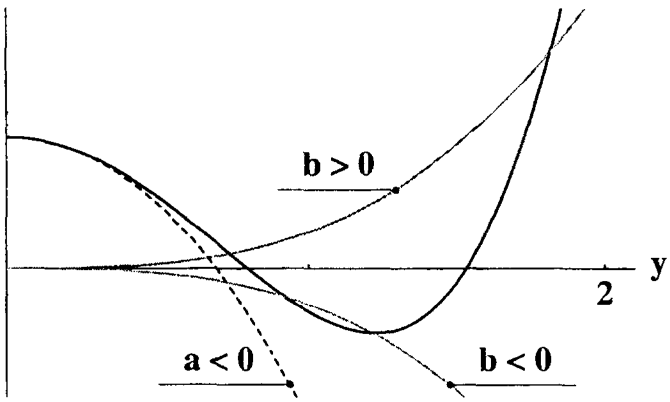

Fig. 6. Representation of Eq. (41a). Observe that in the case $a < 0$, $\sigma C_3 > 0$ only one positive root exists. In the case $\sigma C_3 < 0$ the internal force can be unbounded.

4.2. Periodic wave

Substituting $r^2 = r_3^2 + (r_2^2 - r_3^2)\sin\varphi$, Eq. (19a) is reduced to a transcendental equation relative to $r = r(\xi)$:

$$\sqrt{r_1^2 - r_3^2}\,\frac{\sigma^2}{2}\xi = \pm\left[1 - \frac{\sigma^2}{2}(C_2 - r_1^2)\right]\mathrm{F}(\varphi, k) \mp \frac{\sigma^2}{2}(r_1^2 - r_3^2)\mathrm{E}(\varphi, k), \tag{43a}$$

$$\sqrt{r^2 - r_3^2} = \pm\sqrt{r_2^2 - r_3^2}\,\mathrm{sn}\left[\sqrt{r_1^2 - r_3^2}\,\frac{\sigma^2}{2}\,\frac{\xi + \sqrt{r_1^2 - r_3^2}\,\mathrm{E}(\varphi, k)}{1 - \sigma^2/2(C_2 - r_1^2)}\right], \tag{43b}$$

where

$$\varphi = \arcsin\left(\sqrt{\frac{r^2 - r_3^2}{r_2^2 - r_3^2}}\right), \qquad k^2 = \frac{r_2^2 - r_3^2}{r_1^2 - r_3^2}. \tag{43c,d}$$

In contrast to the case $C_3 = 0$, the solution depends on three constants and cannot be expressed only in terms of the limits of the internal force. It follows from Eq. (40a) that

$$C_2 = \frac{1}{2}\sum_{i=1}^{3} r_i^2, \quad C_2^2 - C_4 = \sum_{i=1}^{3}\sum_{j\neq i}^{3} r_i^2 r_j^2, \quad C_3^2 = \prod_{i=1}^{3} r_i^2, \quad C_3 = \pm\prod_{i=1}^{3} r_i, \tag{44}$$

and hence, from Eqs. (43b) and (8), we obtain (compare with Eq. (30))

$$\eta = \eta_{\max}\,\mathrm{cn}^2\left[\mu\,\frac{|\sigma|\,\xi \pm 2\mu\,\mathrm{E}(\varphi, k)}{1 + f_{\min} - (\sigma^2/2)r_3^2}\right], \tag{45}$$

where

$$\eta = f - f_{\min}; \quad \eta_{\max} = f_{\max} - f_{\min}; \quad \mu = \sqrt{f_{\min} + \eta_{\max}/2 - (\sigma^2/4)r_3^2}.$$

From Eq. (43a), the period of the wave can be expressed as a function of $f_{\max}$, $f_{\min}$ and r_3:

$$|\sigma|\,\frac{L}{2} = \pm\frac{1 + f_{\min} - (\sigma^2/2)r_3^2}{\mu}\,\boldsymbol{K}(k) \mp 2\mu\,\boldsymbol{E}(k). \tag{46}$$

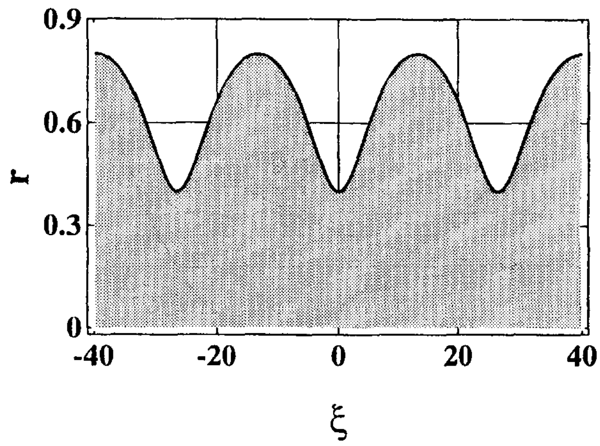

Fig. 7. Radius of the helix in the case $r_0 \neq 0$.

The axial displacement $u(\xi)$ and the angle of rotation $\theta(\xi)$ are then given by the following expressions:

$$u(\xi) = -\xi \cos\gamma + \frac{2C_1}{\sigma^2\sqrt{r_1^2 - r_3^2}}\mathrm{F}(\varphi, k), \tag{47}$$

$$\theta(\xi) = \pm\frac{2\mathrm{F}(\varphi, k)}{\sigma\sqrt{r_1^2 - r_3^2}} \pm \frac{C_3}{r_3^2\sqrt{r_1^2 - r_3^2}}\Pi(\varphi, k, m) - \lambda\xi, \tag{48a}$$

$$\phi(s, \tau) = \pm\frac{2\mathrm{F}(\varphi, k)}{\sigma\sqrt{r_1^2 - r_3^2}} \pm \frac{C_3}{r_3^2\sqrt{r_1^2 - r_3^2}}\Pi(\varphi, k, m) + \sigma\tau, \tag{48b}$$

where

$$\Pi(\varphi, k, m) = \int_0^{\varphi} \frac{\mathrm{d}\varphi}{(1 + m\sin^2\varphi)\sqrt{1 - k^2\sin^2\varphi}} \quad \left(m = \frac{r_2^2 - r_3^2}{r_3^2}\right) \tag{48c}$$

is the normal elliptic integral of the third kind. The radius $r(\xi)$ of the deformed helix is shown in Fig. 7.

4.3. Solitary wave

The solitary wave may be considered as a particular case of the general solution, when two of three roots of Eq. (40) are equal to each other, i.e. $r_1 = r_2$, and the modulus k of the elliptic integrals, given by Eq. (43d), is equal to unity. The expressions for the radius of the helix and for the amplitude of the wave $\eta = f - f_{\min}$ can be obtained from Eqs. (43b) and (45):

$$\sqrt{r^2 - r_3^2} = \sqrt{r_2^2 - r_3^2}\tanh\left[\frac{\sigma^2}{2}\sqrt{r_2^2 - r_3^2}\,\frac{\xi + \sqrt{r^2 - r_3^2}}{1 - \sigma^2/2(C_2 - r_2^2)}\right], \tag{49}$$

$$\eta = \frac{\sigma^2}{2}(r_2^2 - r^2) = \eta_{\max}\operatorname{sech}^2\left[\sqrt{\frac{\eta_{\max}}{2}}\,\frac{|\sigma|\,\xi + \sqrt{2(\eta_{\max} - \eta)}}{1 - f_{\min}}\right], \tag{50}$$

where

$$r_3^2 = \frac{2}{3}C_2 - \frac{2}{3}\sqrt{C_2^2 + 3C_4}, \quad r_2^2 = \frac{2}{3}C_2 + \frac{1}{3}\sqrt{C_2^2 + 3C_4} \qquad (C_4 < 0). \tag{51a,b}$$

We observe that solution (50) depends on two constants, $f_{\max}$ and $f_{\min}$. In the case of the solitary wave, these constants must satisfy the condition $u' = 0$ for $\xi = \infty$; from this condition (see Eq. (6)),

$$C_1 = \cos\gamma(1 - f_{\min}). \tag{52a}$$

From Eq. (52a) and using Eqs. (44), (8b) and (17), we obtain

$$C_1 = \sqrt{\left[1 - \operatorname{sgn}(\sigma C_3)\sqrt{f_{\min}}\right]^2 - 2(f_{\max} + f_{\min})}. \tag{52b}$$

The relation between the amplitude of the wave $\eta_{\max}$ and the force at infinity, $f_{\min}$ has the form

$$\eta_{\max} = \frac{\lambda^2}{2}\left[1 - \operatorname{sgn}(\sigma C_3)\sqrt{f_{\min}}\right]^2 - 2f_{\min}. \tag{52c}$$

As noted above, in the case of the solitary wave we have $f < 1$. Using Eqs. (52b) and (51a,b), we can obtain the limit of the internal force:

$$f_{\max}^{(1)} = \frac{1}{9}\frac{(1 - \sqrt{1+3a})(1 + 2\sqrt{1+3a})}{(1 + \sqrt{1+3a})^2}\left[-\operatorname{sgn}(\sigma C_3) + \sqrt{2}\sqrt{\frac{2 + \sqrt{1+3a}}{1 - \sqrt{1+3a}}}\right]^2, \tag{53}$$

where parameter $a = C_4/C_2^2$ was introduced in Eq. (40c).

Integrating Eq. (6) with condition (52a) and choosing the constant of integration C_6 (see Eq. (19b)) in accordance with the condition $u = 0$ for $\xi = +\infty$, we obtain

$$u(\xi) = \cos\gamma\left[\sqrt{r_2^2 - r_3^2}\operatorname{sgn}\xi - \sqrt{r^2 - r_3^2}\right]. \tag{54}$$

It follows from Eq. (54) that, as in the case $C_3 = 0$, the solitary wave leads to a constant shift in the axial direction.

Thus the solitary wave propagates in the helix under an initial constant force $f_{\min}$ (see Figs. 8(a) and (b)). It is clear that equilibrium is maintained, in this case, by the inertia forces associated with the rigid body rotation of the

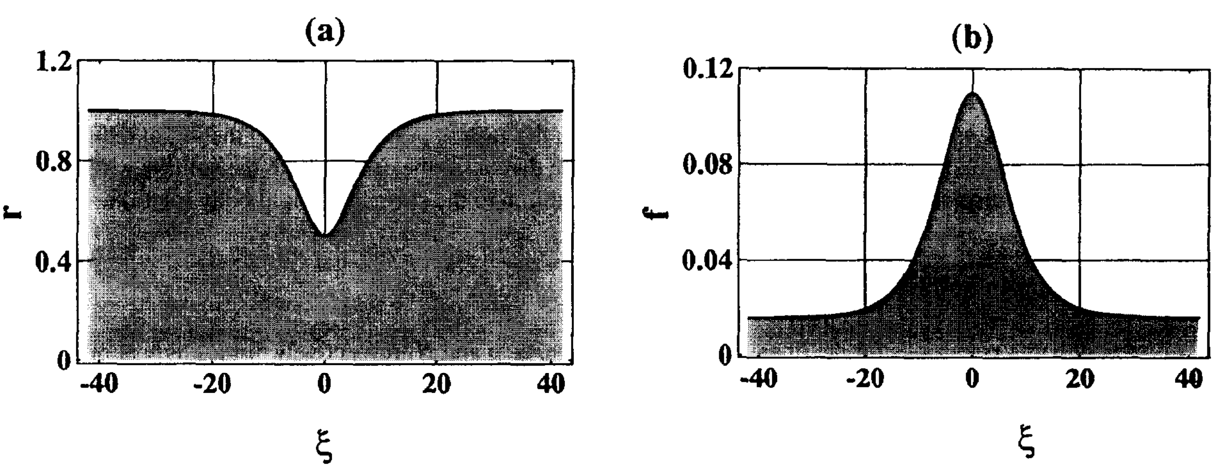

Fig. 8. Solitary wave solution for the case $r_0 \neq 0$: (a) radius of the helix; (b) internal force.

helix. From the representation of the position vector, Eqs. (10a–c) and (12a), it follows that the angular velocity, $\dot{\phi} = -\phi' + \sigma$, at infinity is given by

$$\dot{\phi} = -\frac{\sigma f_{\min}}{1 - f_{\min}} - \frac{\sigma^2}{2} \frac{C_3}{r_2^2 (1 - f_{\min})} \quad (r = r_2), \tag{55}$$

and is not equal to zero. From Eqs. (44) and (8b) it follows that in the case of the solitary wave, $C_3 = \pm r_3 r_2^2$, $r_3 = 2\sqrt{f_{\min}}/|\sigma|$, and the angular velocity at infinity can be expressed as a function of $f_{\min}$:

$$\dot{\phi}_\infty = -\sigma \frac{\sqrt{f_{\min}}}{1 - \sqrt{f_{\min}}} \quad (\sigma C_3 > 0), \tag{56a}$$

$$\dot{\phi}_\infty = \sigma \frac{\sqrt{f_{\min}}}{1 + \sqrt{f_{\min}}} \quad (\sigma C_3 < 0). \tag{56b}$$

From the condition at infinity ($r = r_2$), we find that $\phi' = \lambda$, and from Eqs. (56a,b), we obtain immediately $\theta' = -\dot{\theta} = 0$, and hence

$$\omega = -\lambda \sqrt{f_{\min}} \quad (\sigma C_3 > 0), \tag{57a}$$

$$\omega = \lambda \sqrt{f_{\min}} \quad (\sigma C_3 < 0). \tag{57b}$$

Thus the constant nonzero internal force is a consequence of the rigid body rotation of the undeformed helix. As noted above, the case $\omega = -\lambda$, $f_{\min} = 1$ corresponds to the D'Alembert solution.

It follows from Eqs. (57a,b) that, in the case of the solitary wave, σ is positive and that $\mathrm{sgn}(\sigma C_3) = \mathrm{sgn}(C_3)$. The sign of σC_3 depends on the relationship between the directions of the rotation of the helix and the wave. Thus, as a result of the rigid body rotation of the helix, there is no reflection symmetry: positive and negative directions along the x-axis are not equivalent to each other.

We recall that the effective length of the solitary wave in the case $r_0 = 0$ is independent of the amplitude of the wave and depends only on the parameter λ. However, in the case of the rotating helix, the effective wave length is governed by two parameters: λ and ω. In effect, for $r \to r_2$, we have $\xi \gg \sqrt{\eta_{\max} - \eta}$ and, thus

$$\eta \sim \eta_{\max} \operatorname{sech}^2 \left[\sqrt{\frac{\eta_{\max}}{2}} \frac{|\sigma| \xi}{1 - f_{\min}} \right] \quad (r \sim r_2), \tag{58a}$$

where the amplitude of the wave $\eta_{\max}$ can be expressed as a function of λ and ω (see Eqs. (52c,57)):

$$\eta_{\max} = \frac{\sigma^2}{2} - 2 f_{\min} = \frac{\sigma^2}{2} - 2\frac{\omega^2}{\lambda^2}. \tag{58b}$$

Eq. (58a) can also be considered as the asymptotic solution for the case of a small amplitude, $\eta_{\max} \ll 1$.

It follows from Eqs. (58b), (51) and (8), that (similarly as in the case $r_0 = 0$, and $r_2 = 1$) the initial radius of the helix is restored after the wave has passed. Further, we observe that, as in the case $r_0 = 0$, the solitary wave causes finite nonzero axial displacements and angular rotations in addition to the permanent rigid body rotation.

5. Integral properties of the solution

We present here expressions for the linear and angular momenta, $\boldsymbol{p}$ and $\boldsymbol{H}$, respectively, for a single period of the wave. From Eqs. (22) and (4), it follows that $\dot{\boldsymbol{r}}_x = -u' \boldsymbol{k}_x$ and hence the axial momentum is

$$\boldsymbol{p} = -2\rho v R_0 \int_0^{L/2} u'(\xi)\, \mathrm{d}\xi \boldsymbol{k}_x = -2\rho v R_0 \left[u\left(\frac{L}{2}\right) - u(0) \right] \boldsymbol{k}_x. \tag{59}$$

Since the velocity of rotation is $\dot{\phi}(\xi) = -\phi'(\xi) + \sigma$, the angular momentum is

$$\boldsymbol{H} = -2\rho v R_0^2 \int_0^{L/2} r^2(\phi' - \sigma)\,\mathrm{d}\xi. \tag{60}$$

We note that these relations lead to expressions for the axial and angular momenta in terms of complete elliptic integrals.

In the case of the solitary wave, for which the helix is at rest at infinity ($r_0 = 0, \omega = 0$), the expressions for the axial and angular momenta were obtained in [2]:

$$\boldsymbol{p} = -2\rho v R_0 \cos\gamma\, \boldsymbol{k}_x, \qquad \boldsymbol{H} = -\tfrac{2}{3}\rho v R_0^2 \sin\gamma\, \boldsymbol{k}_x. \tag{61a,b}$$

Using Eqs. (59) and (54), we find the axial momentum for the solitary wave in the rotating helix:

$$\boldsymbol{p} = -2\rho v R_0 \cos\gamma \sqrt{r_2^2 - r_3^2} = -2\rho v R_0 \frac{\cos\gamma}{|\sin\gamma + \omega|} \sqrt{2\eta_{\max}}. \tag{62}$$

The rotation of the helix at infinity does not permit one to determine readily the angular momentum using Eq. (60). However, excluding the rotation of the helix as a rigid body with angular momentum $\boldsymbol{H}_\infty$, we obtain

$$\Delta\boldsymbol{H} = \boldsymbol{H} - \boldsymbol{H}_\infty = -2\rho\, v\, R_0^2 \int_0^{L/2} \{r^2(\phi'(r) - \sigma) - r_2^2(\phi'(r_2) - \sigma)\}\,\mathrm{d}\xi, \tag{63}$$

where (see Eqs. (12) and (14))

$$\Delta\boldsymbol{H} = -\frac{4}{3}\rho v R_0^2 \sin\gamma \frac{\sqrt{2\eta_{\max}}}{\sigma^3}\left[3 f_{\min} + \eta_{\max} + \mathrm{sgn}(C_3)\sqrt{f_{\min}}(3 f_{\min} + 2\eta_{\max})\right]. \tag{64}$$

6. Conclusions

The solutions described above correspond to traveling, propagating-rotating waves. These solutions describe various types of solitary and periodic nonlinear waves in an inextensible flexible helical fiber. The waves can be separated into two types. In the wave of the first type, there exists a point where the fiber crosses the axis of the helix. The effective length of the solitary wave, in this case, does not depend on the amplitude of the wave and is defined only by the pitch of the undeformed helix.

In the wave of the second type, the fiber does not cross the axis of the helix. The solitary wave of the internal force propagates as a disturbance to an initial nonzero internal force which is a result of the rigid body rotation of the helix. The effective length of the solitary wave, in this case, is dictated by the pitch of the helix and by the angular velocity of the rigid body rotation. The reflection symmetry does not hold in this case, and parameters of the solitary wave depend on the direction of the propagation.

The solitary waves, in both cases, cause finite nonzero shifts in the axial displacement and rotation, but the initial shape is restored. In the case of the periodical wave, nonzero axial and angular averaged velocities arise as a result of such shifts (Fig. 9). In the asymptotic case of small amplitude, the periodic wave appears as a sinusoidal wave.

Note that, in addition to the traveling-wave solutions considered, some results of a numerical simulation of transient problems have been obtained. A discretized system was considered as a chain of masses connected to each other by inextensible, massless links [20]. A comparison with the analytical solution reveals that the wave shape and velocity correspond to the theoretical data with very high accuracy and that no disturbances exist outside the "effective support" of the wave. An examination of stability of the derived analytic solution was also performed in

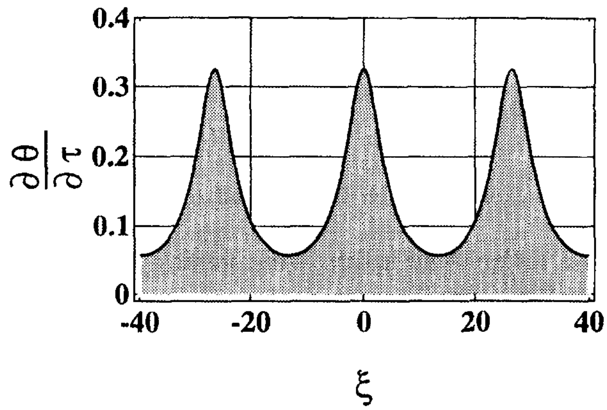

Fig. 9. Periodic component of the angular velocity in the case $r_0 \neq 0$.

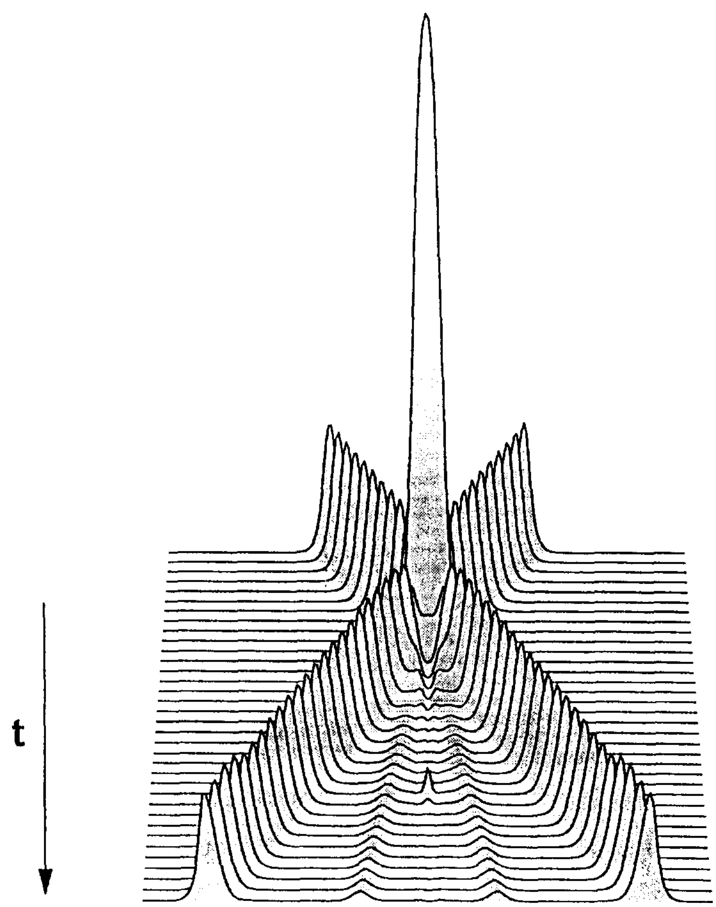

Fig. 10. Collision of two solitary waves propagating in opposite directions.

[20].[6] Collisions of two solitary waves were considered numerically as well. Although the solitary waves obtained by the numerical simulation propagate as very stable objects, the collisions appear to be not perfectly elastic. After the collisions the main waves continue to propagate as solitary waves, but the amplitudes change with respect to the values before the collision. In the specific case of collision of two identical waves which propagate in opposite directions, the amplitudes of both decrease, and small additional solitary waves are created. Such a collision of the waves in the helix which is at rest at infinity is shown in Fig. 10.

The question arises: what is the cause of the energy radiation due to the collision? We should first note that we encounter a new phenomenon: in contrast to the traditional consideration of soliton propagation, in a certain sense, a change of the waveguide occurs in the considered system after the wave has passed; namely, a finite shift, $u = -2\cos\gamma$, appears in the axial displacement and $\phi = -2\sin\gamma$ in the rotation. More specifically, recalling that the phenomenon of wave propagation in the helix is a vector phenomenon, we note that several quantities are associated with the wave: force, F; radius of the helix change, $|\boldsymbol{R}| - R_0 = R_0(|r| - 1)$; axial displacement, u; and angle change, $\phi - \lambda s$. While the first two, force and radius change, appear as solitary disturbances, a constant, nonvanishing, shift occurs in the axial displacement and angle change as is mentioned above, resulting in an altered waveguide. The presence of these last two disturbances may be the reason for the energy radiation. In effect, the propagation of waves after collision requires their "perestroika" to satisfy these new conditions. In the case of collision of two solitary waves propagating in the same direction, the weaker wave propagates (slower than the stronger one) in the undisturbed helix before the collision but in the tail of the stronger one after the collision, while the opposite is true for the stronger wave. In the case of two waves propagating in opposite directions, both waves propagate initially in the undisturbed helix before the collision and in the disturbed helix after the collision. In spite of such energy radiation, the results show that the post-collision wave is formed as a very stable object governed by the given analytical description.

Acknowledgements

This research was supported by grant no. 94-00349 from the United States–Israel Binational Science Foundation (BSF), Jerusalem, Israel, and grant no. 9673-1-96 from the Ministry of Science, Israel, and by The Colton Foundation, USA.

References

[1] H.F. Weinberger, A First Course In Partial Differential Equations, Blaisdell, New York, 1965.
[2] L. Slepyan, V. Krylov, R. Parnes, Solitary waves in an inextensible, flexible, helicoidal fiber, Phys. Rev. Lett. 74 (1995) 2725–2728.
[3] O.B. Gorbacheva, L.A. Ostrovsky, Nonlinear vector waves in a mechanical model of a molecular chain, Physica D 8 (1983) 223–228.
[4] S. Cadet, Propagation and interaction of nonlinear shear waves in a discrete lattice, Wave Motion 11 (1989) 77–97.
[5] Ph. Rosenau, Quasi-continuous spatial motion of a mass–spring chain, Physica D 27 (1987) 224–234.
[6] I.I. Kolodner, Heavy rotating string–a nonlinear eigenvalue problem, Commun. Pure Appl. Math. 8 (1955) 344–408.

[6] Transient problems were considered numerically for Eq. (1) with initial conditions which correspond to the theoretical solitary wave as found analytically. It was established that the solitary wave obtained by this numerical simulation propagates as a very stable object and only a very low dissipation caused by the discretization was detected. Furthermore, the stability with respect to a finite perturbation was studied by modeling the formation of the wave from an arbitrary initial disturbance. This initial disturbance leads to a set of stable solitary waves which conform to the theoretical description. Axial dynamic tension of a semi-infinite helical fiber was studied numerically in [21] and was found to lead to an extraordinary nonlinear "binary" wave consisting of quasi-periodical propagating waves for both the $f < 1$ and $f > 1$ cases. The structure and velocity of these quasi-periodic waves are in good accordance with analytical results given in the present paper. While an analytic study of the stability of waves, using the formalism given in [23] could be made (and is worthy as a topic of a separate investigation), the numerical studies mentioned above reveal, in themselves, the stability of the analytic solutions obtained in this paper.

[7] M. Reeken, Classical solutions of the chain equation, I, Math. Zeitschrift 165 (1979) 143–169; II, Math. Zeitschrift 166 (1979) 67–82.
[8] S.S. Antman, M. Reeken, The drawing and whirling of strings: Singular global multiparameter bifurcation problems, SIAM J. Math. Anal. 18 (1987) 337–365.
[9] J.B. Keller, Large amplitude motion of a string, Am. J. Phys. 27 (1959) 584–586.
[10] S.S. Antman, The equations for the large vibrations of strings, Am. Math. Monthly 87 (1980) 359–370.
[11] J.E. Peters, W.F. Ames, Group properties of the non-linear dynamic equations of elastic strings, Int. J. Non-Linear Mech. 25 (1990) 107–115.
[12] Ph. Rosenau, M.B. Rubin, Some nonlinear three-dimensional motions of an elastic string, Physica D 19 (1986) 433–439.
[13] S.S. Antman, Nonlinear Problems of Elasticity, Springer, New York, 1995.
[14] L.I. Slepyan, V.I. Krylov, Ph. Rosenau, Solitary waves in a flexible, arbitrary elastic helix, submitted.
[15] V.I. Krylov, Ph. Rosenau, Solitary waves in an elastic string, Phys. Lett. A 217 (1996) 31–42.
[16] A. Cardou, C. Jolicoeur, Mechanical models of helical strands, Appl. Mech. Rev. 50 (1997) 1–14.
[17] V. Beletsky, E. Levin, Dynamics of Space Tether Systems, Main Editorial Board for Physical and Mathematical Literature, Nauka, Moscow, 1990 (in Russian).
[18] A. Cherkaev, L. Slepyan, Waiting element structures and stability under extension, Int. J. Dam. Mech. 4 (1995) 58–82.
[19] L.I. Slepyan, V.I. Krylov, R. Parnes, Solitary and periodical nonlinear waves in a helix, in: B. Tabarrok, S. Dost (Eds.), Proceedings of the 15th Canadian Congress of Applied Mechanics, University of Victoria, vol. 2, 1995, pp. 992–993.
[20] L.I. Slepyan, V.I. Krylov, R. Parnes, Solitary waves in a helix, Proc. Estonian Acad. Sci.: Phys. Math. 44 (1995) 29–39.
[21] V.I. Krylov, L.I. Slepyan, Binary wave in a helical fiber, Phys. Rev. B 55 (1997) 14 067–14 070.
[22] G.B. Whitham, Linear and Nonlinear Waves, Wiley, New York, 1974.
[23] G. Iooss, Bifurcation of a periodic solution of the Navier–Stokes equations into an invariant torus, Arch. Rati. Mech. Anal. 58 (1975) 35–56.